Hindawi Publishing Corporation
Science and Technology of Nuclear Installations
Volume 2015, Article ID 571547, 6 pages
http://dx.doi.org/10.1155/2015/571547

Research Article

The Effects of the Treatment of the Periodic Boundary Condition in TRIAINA Codes with a Pressure Tube Creep Problem

E. H. Ryu,[1] S. Y. Yoo,[2] B. Y. Chung,[1] and J. Y. Jung[1]

[1]*Korea Atomic Energy Research Institute, Daejeon 305-353, Republic of Korea*
[2]*Seoul National University, Seoul 151-744, Republic of Korea*

Correspondence should be addressed to E. H. Ryu; ryueh@kaeri.re.kr

Received 1 October 2014; Revised 26 January 2015; Accepted 6 February 2015

Academic Editor: Bo Wook Rhee

To verify the periodic boundary condition (PBC) treatment which was implemented in a TRI-angle elements induced numerical analyzer (TRIAINA), the pressure tube creep problem is chosen and examined with three cases of normal, 2.5% creep, and 5.0% creep on the aspects of the multiplication factor and relative pin power. The McCARD code is used for the homogenized group constants generation. It is shown that the differences are nearly negligible for the pressure tube creep problem.

1. Introduction

The pressure tube deformation including creep and sagging is an important phenomenon related to nuclear power plant (NPP) aging (Jung, 2011) [1]. It results in the power derating of an NPP because it reduces the thermal margin of the CANDU system. It also affects the neutronic economy of the core. To evaluate and assess the neutronic effects of the pressure tube creep exactly, several quantitative researches are performed. Ilas [2] calculated the multiplication factor and pin power distribution changes with HELIOS. Kim et al. [3] also calculated the multiplication factor and pin power distribution changes depending on the burn-up with the HELIOS code. These researches also include the plutonium generation and void reactivity changes with burn-up. However, those researches have drawbacks that they only dealt with the creep in a two-dimensional space. The sagging effect and global core effect from summing up the individual lattice have never been evaluated precisely.

The SHAFE code (Ryu and Joo, 2013) [4] is based on the finite element method (FEM) and it accepts the general geometry from tetrahedral mesh generators. However, to treat the pressure tube creep in the lattice level, the PBC treatment should be used; thus, it should be tested first. The PBC is boundary condition which is often used to approximate the large system with small cells. But it is different with the reflective boundary condition (RBC). For 2-dimensional space, we realize that the usual pin cell problem gives no difference between result with RBC and result with PBC because the center of the pin cell is positioned right at the center of the cell. If a point is positioned arbitrarily in the cell, the RBC copies it and locates it to a symmetric position about geometric element such as a point, line, and surface with RBC while the PBC copies it and locates it to a same position about geometric element with PBC as illustrated in Figure 1. To verify the methodology for the PBC treatment in FEM, the TRIAINA code which is a 2-dimensional version of the SHAFE code is tested for several cases. In this research, the calculation ability of the PBC implemented in the TRIAINA code is verified with the multiplication factor and relative pin power distribution changes. Three cases of normal, 2.5% creep, and 5.0% creep are discussed with two separate versions of the TRIAINA codes, which are based on the target governing equations of P1 and SP3.

For the TRIAINA code calculation, homogenized cross sections for internal regions of the lattice cell tube are necessary. The McCARD code is used for the homogenized cross section calculation. For the nonfissionable regions,

the sign of absorption cross sections sometimes becomes negative. Because of the large value of $(n, 2n)$ and $(n, 3n)$, the cross section adjustment for the source and loss term balance is not performed to make the sign of the absorption cross sections positive in this research. Thus, the cross sections used here are somewhat larger than the actual values.

The geometry is based on the fresh fuel dimensions specified in the PDM report [5]. The half lattice cell is used, and the geometry modelling and the meshing are done with the GMSH generator [6]. To see the effect of the second order basis function, the number of unknowns is almost the same as the number of unknowns in the case of a linear basis function. For the use of the second-order basis function, a full mapping option is selected for all cases in the selective mapping scheme.

2. Group Constant Generation

The TRIAINA code only accepts homogenized cross section for each region. The McCARD code and the ENDF 7.0 library are used for homogenized cross section generation with the critical spectrum of the reference fresh fuel design. To obtain the fine group spectrum of each region, a Monte Carlo simulation is performed with a million particles and one-thousand cycles including 200 inactive cycles. To obtain the diffusion coefficient and critical spectrum, the B_1 equation for homogenized system is solved. It is assumed that the cross sections do not change when the creep occurs [7].

Two group cross sections for regions are generated with the energy boundary of 0.625 eV. As mentioned in paragraph 3 of Section 1, the absorption cross section becomes negative if the (n, Xn) cross section is included. Because the McCARD code does not accept negative cross section, it is impossible to exclude the (n, Xn) cross section from absorption cross section [8]. Thus, the source term correction should be done in the RFSP and TRIAINA code, in principle. However, in this research, the main objective is to see the difference between results using different boundary conditions. Thus, the source term correction is not done.

3. CANDU Bundle Geometry

The reference data are taken from the physics design manual [5]. The fuel rod geometry including the pellet, gap, and cladding is simplified to one fissionable region. The fuel rod cross sections are distinguished by the distance from the centre of the lattice. Thus there are a total of 9 identical regions including fuel array 1, fuel array 2, fuel array 3, fuel array 4, coolant, a pressure tube, a gap, a calandria tube, and a moderator.

The GMSH utility is used for both modelling and meshing for all cases. For the modelling of the creep case, the boundary between the coolant and pressure tube is determined by two ellipses. In the case of 5.0% creep, one ellipse has a major axis of 105% and a minor axis of 102.5% relative to the pressure tube inner radius. The other ellipse has a major axis of 102.5% and a minor axis of 100% relative to the pressure tube inner radius as depicted in Figure 2 [3]. In addition, the area with a grey color indicates the increased coolant region because of creep. Figure 2 shows 5% creep case, 2.5% creep case, and normal case from the left. For the case of a linear basis function, about 5,400 nodes and 10,000 triangle elements are used. For the case of a quadratic basis function, about 5,400 nodes and 2,600 elements are used. And the enlargement of the geometry modelling on creep area is also shown in Figure 3. Because of the large volume of the moderator, the creep area in real scale is not easy to verify the creep area clearly. The number of creeps in percent means that the increased size for y-direction is the relative ratio about radius of the inner radius of the pressure tube.

The mesh generation for the different basis functions is done by conserving the number of unknowns. Because the linear mapping cannot preserve the area of the fuel region, the result using a quadratic basis function with full mapping is more reliable although the average pitch of the linear basis function case is half that of the quadratic basis function, as shown in Table 1.

Table 1: Average pitch of triangle elements.

	Normal	2.5% creep	5.0% creep
Linear Ftn.			
PBC	0.173 cm	0.172 cm	0.173 cm
RBC	0.173 cm	0.172 cm	0.173 cm
Quadratic Ftn.			
PBC	0.346 cm	0.344 cm	0.345 cm
RBC	0.347 cm	0.343 cm	0.344 cm

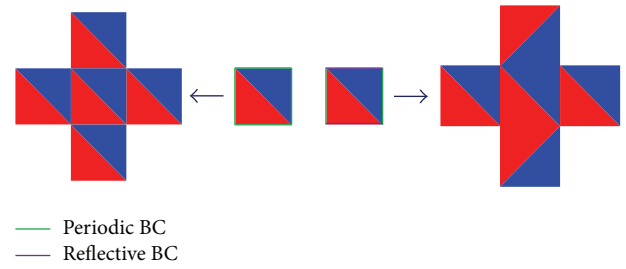

Figure 1: Comparison of the PBC and RBC. Implementation of the periodic boundary condition: (i) difference of periodic BC and reflective BC and (ii) physical interpretation. (a) Because the same structure is repeated for the periodic BC, the flux values of the same position on the every line on the periodic BC are the same. (b) Because the GMSH gives the same coordinates for the nodes on the periodic boundary condition, the implementation of the periodic BC is much easier.

4. Fundamentals of the Implementation of the PBC

The mathematical explanation of the PBC is the same flux condition for the corresponding lines of the BC. In the case of the y-directional PBC as the pressure tube creep problem, the coordinate of the x-axis of nodes on the corresponding lines is the same if the GMSH utility is used. Thus, the flux of corresponding nodes should be the same. This is quite similar

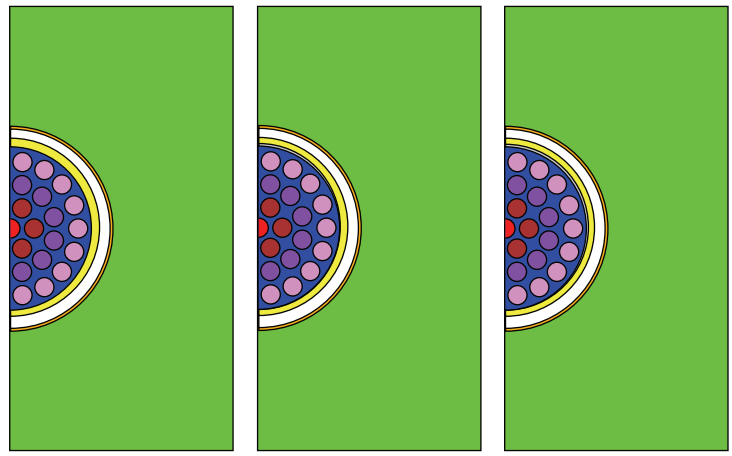

Figure 2: Geometry modelling.

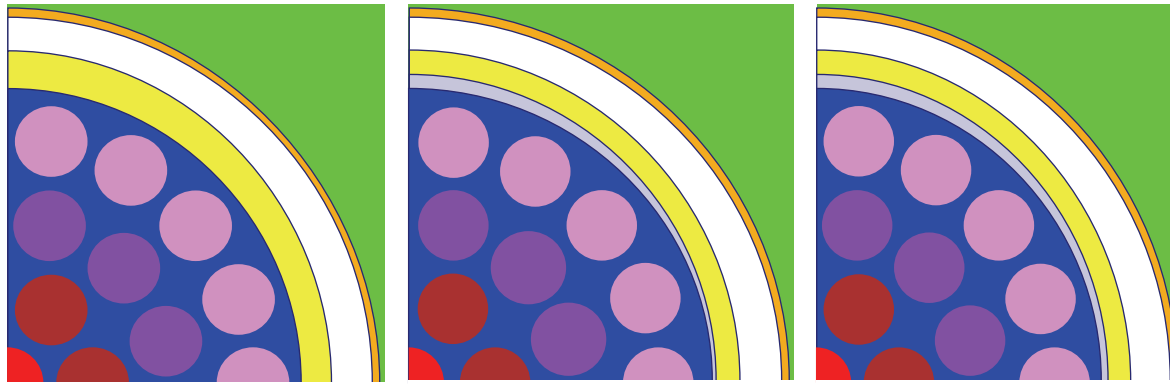

Figure 3: Enlargement of the geometry modeling.

with the mathematical interpretation of the rotational BC. By assigning the same indices to the corresponding two nodes which have the same coordinate, the PBC can be reflected. In this research, a general situation including different values of the coordinate of the x-axis is not considered thanks to the GMSH utility.

5. Numerical Results

The multiplication factors in pcm for both P1 and SP3 are listed in Tables 2 and 3. It is verified that the results of RBC and PBC are the same for all cases. In the results of multiplication factors, the difference from the different boundaries cannot be distinguished at all in the pcm level.

In Tables 2 and 3, the quadratic basis function and mapping effects are well revealed for every case. As the creep value increases, it is observed that the multiplication factor decreases linearly, and the amount of increment is about 110 pcm. It can be also expected and verified that the transport effect in the CANDU bundle problem is very large. We can confirm that the difference between the results of P1 and SP3 is 1,000 pcm for every case for the multiplication factor. Thus, it is expected that the difference between solutions of the diffusion equation and Boltzmann transport equation is much larger than 1000 pcm. Also, the large transport effect can be a rationale for the use of the transport code in the lattice calculation. The McCARD code solution of the multiplication

Table 2: Multiplication factors of the TRIAINA-P1 code.

	Normal	2.5% creep	5.0% creep
Linear Ftn.			
Periodic BC	1.12206	1.12098	1.11992
Reflective BC	1.12206	1.12098	1.11992
Quadratic Ftn.			
Periodic BC	1.11891	1.11782	1.11677
Reflective BC	1.11891	1.11782	1.11677

Table 3: Multiplication factors of the TRIAINA-P3 code.

	Normal	2.5% Creep	5.0% Creep
Linear Ftn.			
Periodic BC	1.11227	1.11114	1.11005
Reflective BC	1.11227	1.11114	1.11005
Quadratic Ftn.			
Periodic BC	1.10894	1.10781	1.10673
Reflective BC	1.10894	1.10781	1.10673

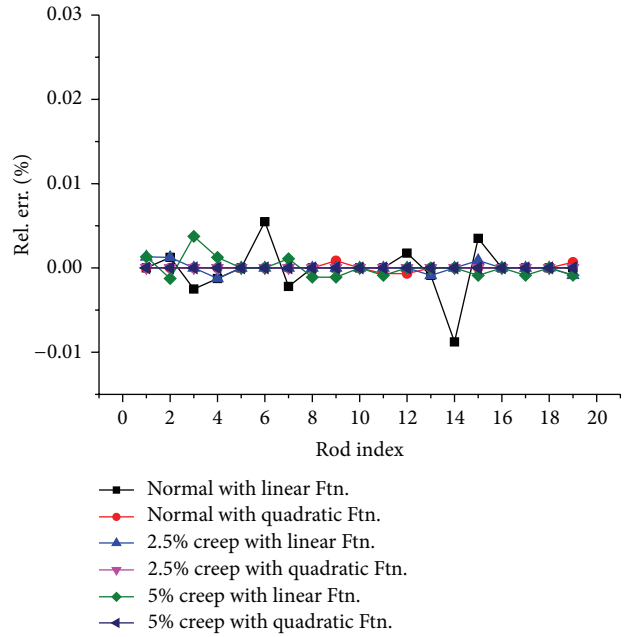

Figure 4: Relative pin power errors with different BCs of the TRIAINA-P1 code.

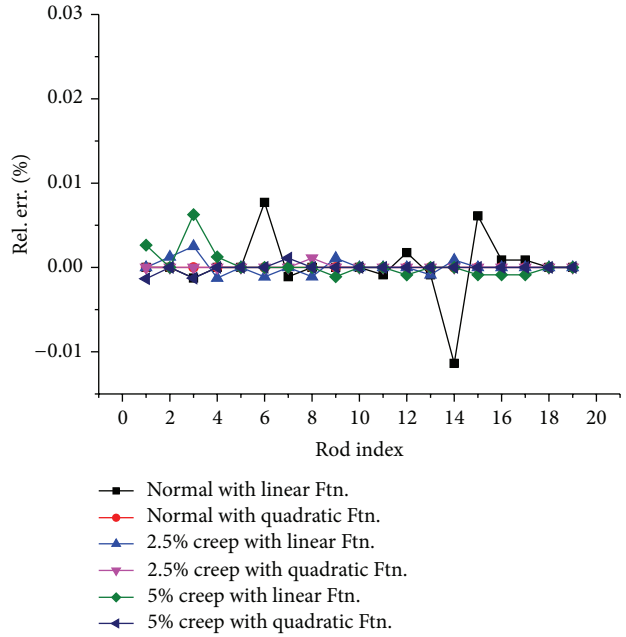

Figure 5: Relative pin power errors with different BCs of the TRIAINA-SP3 code.

factor for the normal case is 1.10377 with two million particles and 1,000 cycles including 200 inactive cycles.

To see the difference between different two boundary conditions, the pin power result should be investigated. In Figures 4 and 5, the relative power errors for 19 pins to the reference power using RBC are plotted and it can be verified that all the relative errors lie on the interval between −0.02% and 0.01%. Because the size of the errors is extremely small, it can be said that the result using the PBC is almost the same as the result using the RBC. Because the verification of the TRIAINA code is done for the reflective boundary, it can be said that there is no problem to use the RBC instead of the PBC for the pressure tube creep problem.

As shown in Figures 4 and 5, the relative pin power errors for different boundary conditions are nearly negligible for all cases as was the case for the multiplication factors. By considering that the reference pin power is close to the 1, the magnitude of the pin power error is order of 10^{-4}. Also, it

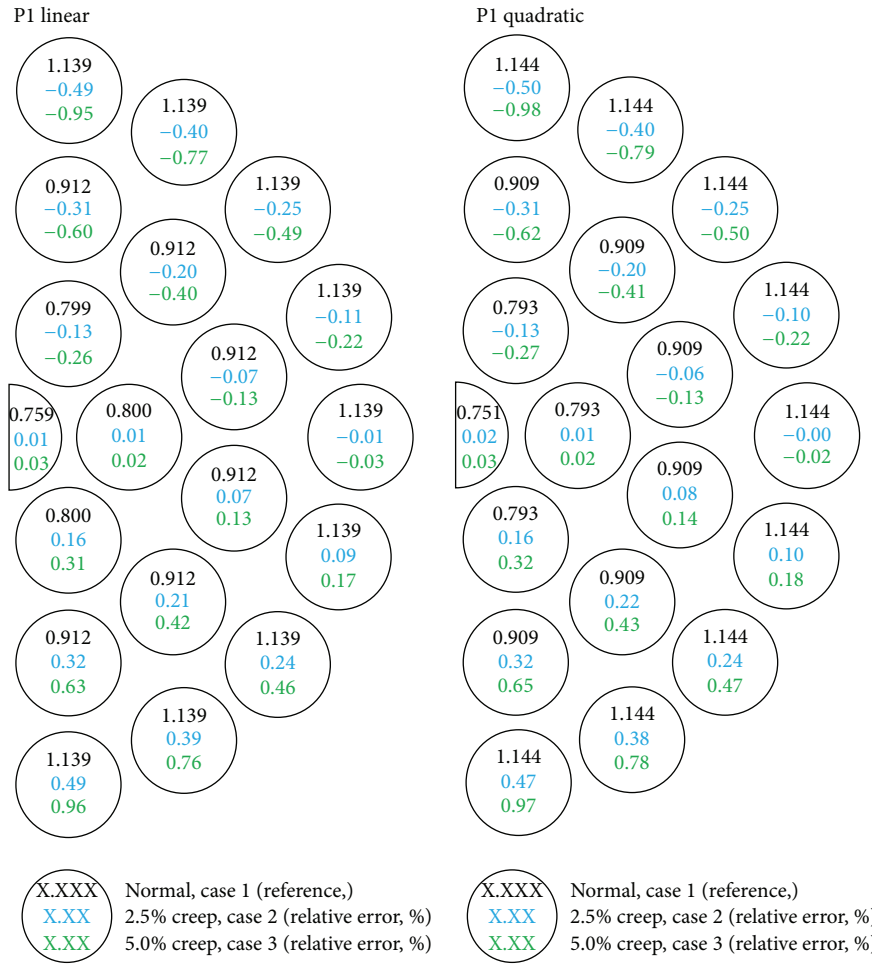

Figure 6: Relative errors of pin power with creep of the TRIAINA-P1 code.

is revealed that the relative pin power is independent of the order of basis function, the degree of creep, and the target governing equation. This fact can be used also for the 3-dimensional calculation of the pressure tube creep problem. And it is not necessary to use the transport code such as MCNP which allows the usage of the PBC for the reference calculation for the pressure tube problem.

In Figures 6 and 7, the left figure is the result of linear basis function and the right figure is the result of quadratic basis function. Every result indicates that the pin powers in upper quarter circle are decreasing when the creep occurred while the pin powers in the remained quarter circle are increasing. Note that the pin index starts from the inner ring to most outer ring and increases with clockwise direction. Thus the pin powers which have indices of 2, 5, 6, 7, 11, 12, 13, and 14 are decreased with the degree of creep.

The linearity of the multiplication factor is showed again for the relative errors of pin powers for every result in Figures 6 and 7. It is expected that relative error of pin power for 7.5% creep case will be three times larger than that for 2.5% creep case. But case with degree of creep more than 5% is not dealt with in this research because it does not appear in the real station in the permitted operation period [1].

6. Conclusions

In this research, it is shown that the difference between used different boundary conditions is negligible for the pressure tube creep problem by investigating multiplication factors and relative errors of pin power by using the TRIAINA code and the McCARD code. The differences of the multiplication factors are zero in pcm level and the relative errors of pin power are nearly negligible for all cases. Thanks to the GMSH utility, realization and implementation of PBC were possible.

This fact enables the usage of the McCARD code for the reference result generation even for the three-dimensional space. This work is a start for exact evaluation of effects of the three-dimensional pressure tube aging including the creep and the sagging and integrated core. Although it is revealed that the reflective boundary can be used for the pressure tube problem, it seems that the exact derivation for the periodic boundary for the three-dimensional space is needed for the general usage for the SHAFE code for the future. Also, for the investigation of the effects of pressure tube aging and integrated core, the general CAD modelling is required. Particularly for the integrated core effect, the parallelization of the SHAFE code is the work of first priority.

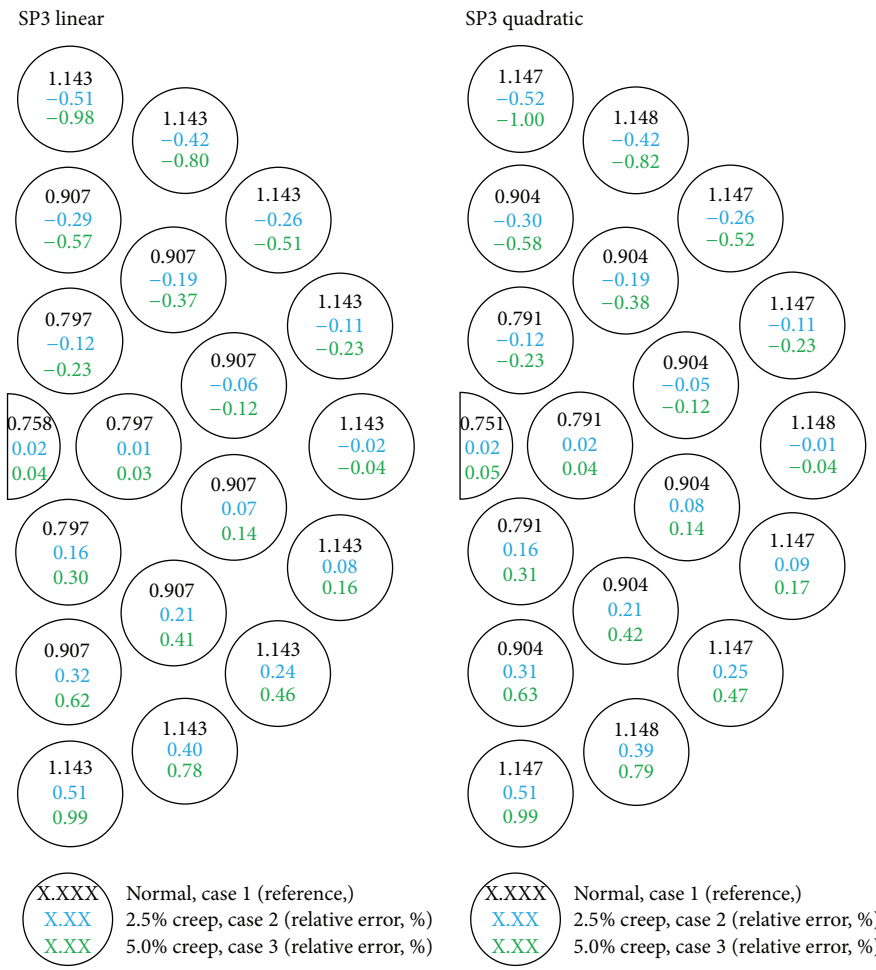

Figure 7: Relative errors of pin power with creep of the TRIAINA-SP3 code.

Conflict of Interests

The authors declare that there is no conflict of interests regarding the publication of this paper.

Acknowledgment

This work was supported by the National Research Foundation of Korea (NRF) Grant funded by the Korea government (Ministry of Science, ICT, and Future Planning) (no. NRF-2012M2A8A4025966).

References

[1] J. Y. Jung, "A development of evaluating model of crept pressure tube diameter for CANDU reactor," Tech. Rep. RR-3497, Korea Atomic Enery Research Institute, Daejeon, Republic of Korea, 2011.

[2] G. Ilas, "Impact of pressure tube aging on physics parameters of a CANDU lattice cell," in *Proceedings of the Advances in Nuclear Fuel Management III (ANFM '03)*, Hilton Head Island, SC, USA, October 2003.

[3] H. S. Kim, G. H. Roh, Y. H. Kim, and J. H. Park, "Neutronics impact of pressure tube creep in a CANDU lattice," Tech. Rep. TR-3701, KAERI, 2008.

[4] E. H. Ryu and H. G. Joo, "Finite element method solution of the simplified P_3 equations for general geometry applications," *Annals of Nuclear Energy*, vol. 56, pp. 194–207, 2013.

[5] KHNP, "Design Manual," CANDU 6 Generating Station Physics Design Manual, Wolsong NPP 1, 59RF-03310-DM-000 Revision 0, 2011.

[6] C. Geuzaine and J.-F. Remacle, "Gmsh: a three-dimensional finite element mesh generator with built-in pre- and post-processing facilities," *International Journal for Numerical Methods in Engineering*, vol. 79, no. 11, pp. 1309–1331, 2009.

[7] S. Y. Yoo and H. J. Shim, "Monte Carlo few group constant generation for CANDU reactor core analysis," in *Transaction of the Korean Nuclear Society Autumn Meeting*, Gyeongju, Republic of Korea, October 2012.

[8] H. J. Shim, B. S. Han, J. S. Jung, H. J. Park, and C. H. Kim, "McCARD: Monte Carlo code for advanced reactor design and analysis," *Nuclear Engineering and Technology*, vol. 44, no. 5, pp. 161–176, 2012.